Analytic 1-D pn Junction Diode Photocurrent Solutions Following Ionizing Radiation and Including Time-Dependent Changes in the Carrier Lifetime From a Nonconcurrent Neutron Pulse

Carl L. Axness, Bert Kerr, and Eric R. Keiter, *Member, IEEE*

***Abstract*—Circuit simulation codes, such as SPICE, are invaluable in the development and design of electronic circuits in radiation environments. These codes are often employed to study the effect of many thousands of devices under transient current conditions. Device-scale simulation codes are commonly used in the design of individual semiconductor components, but computational requirements limit their use to small-scale circuits. Analytic solutions to the ambipolar diffusion equation, an approximation to the carrier transport equations, may be used to characterize the transient currents at nodes within a circuit simulator. We present new analytic transient excess carrier density and photocurrent solutions to the ambipolar diffusion equation for 1-D abrupt-junction pn diodes. These solutions incorporate low-level radiation pulses and take into account a finite device geometry, ohmic fields outside the depleted region, and an arbitrary change in the carrier lifetime due to neutron irradiation or other effects. The solutions are specifically evaluated for the case of an abrupt change in the carrier lifetime during or after, a step, square, or piecewise linear radiation pulse. Noting slow convergence of the Fourier series solutions for some parameters sets, we evaluate portions of the solutions using closed-form formulas, which result in a two order of magnitude increase in computational efficiency.**

***Index Terms*—Ambipolar diffusion equation, finite Fourier transform, neutron irradiation, transform techniques, transient radiation effects.**

I. Introduction

TRANSPORT behavior of excess carriers in semiconductors is described by the equations of current and continuity for electrons and holes as well as Poisson's equation, which relates the electric field and net charge density. For each carrier, the current equation may be substituted into the continuity equation, resulting in three equations describing carrier transport [1, pp. 320–327]. The three resulting equations are not amenable to exact analytic mathematical techniques. The electrical neutrality or charge balance approximation suggested by Van Roosbroeck [2] is used to combine the electron and hole current-continuity equations into the single ambipolar diffusion equation (ADE) [1, pp. 327–328]. The electrical neutrality approximation states that the excess electron and hole densities are equal everywhere within the device. The parameters of the resulting approximate equation are the ambipolar diffusion parameters, as described in Table I. The electric field in the ambipolar diffusion equation includes an external field imposed by a voltage bias applied at the device contacts and an internal field set up by the charged particles within the device.

Analytic mathematical models [3], [4] have been developed over the past four decades that predict transient radiation-induced photocurrents due to excess carrier generation in 1-D pn junction diodes, and have often been the basis for compact device models used in circuit simulation. These models are generally applicable under limited boundary conditions with restrictions on the carrier generation rate. An early transient radiation effects model is that of Wirth–Rogers [3], which describes the current density solution to the ambipolar diffusion equation for a semi-infinite 1-D pn junction diode with no ohmic field in the undepleted region. Stuetzer [4] examined the steady-state behavior of a diode under radiation and found the excess carrier and current densities for a diode of finite extent. Work by Axness, Kerr, and Wunsch [5] extended the solution to monochromatic light pulses and found an n-dimensional transformation from the ADE to the nonhomogeneous heat equation. This paper generalizes the solutions of [5] to the particular case of a time-dependent change in the carrier lifetime during or after irradiation. This behavior might be expected for a neutron pulse that is not coincident with the device irradiation. The mathematical solutions presented here can form the basis for a compact model of combined (neutron and gamma) radiation effects. These compact models are the backbone of circuit simulation codes and enable qualification of rad-hard circuit designs.

The effect of neutron damage to semiconductor devices has been studied by a number of authors (see [6] for review). Neutrons and other high-energy particles collide and displace lattice atoms in semiconductors, creating Frenkel defects. Primary displaced atoms typically have enough energy to create secondary defects. These vacancies may combine with dopant and impurity atoms to form stable defects, which, in turn, may serve as

Manuscript received July 16, 2010; revised August 31, 2010; accepted September 02, 2010. Date of current version December 15, 2010. This work was supported by the QASPR Program at Sandia National Laboratories.

Sandia National Laboratories is a multi-program laboratory managed and operated by Sandia Corporation, a wholly owned subsidiary of Lockheed Martin Corporation, for the U.S. Department of Energy's National Nuclear Security Administration under Contract DE-AC04-94AL85000.

C. L. Axness and E. R. Keiter are with the Sandia National Laboratories, Albuquerque, NM 87185-0779 USA (e-mail: claxnes@sandia.gov; erkeite@sandia.gov).

B. Kerr is with the Mathematics Department, New Mexico Institute of Mining and Technology, Socorro, NM 87801 USA (e-mail: kerr@nmt.edu).

Color versions of one or more of the figures in this paper are available online at http://ieeexplore.ieee.org.

Digital Object Identifier 10.1109/TNS.2010.2086484

TABLE I
DEFINITION AND DESCRIPTION OF IMPORTANT PHYSICAL CONSTANTS AND PARAMETERS

Parameter	Description/Equation/cgs units
a	$\mu_p E_n/2D_p$ (1/cm)
E, E_p, E_n	Ohmic electric field in undepleted zone (V/cm)
$J(t), J_{p\text{ or }n}(t)$	Undepleted zone current densities (A/cm^2)
$n\,(x,t)$	electrons per unit volume (1/cm^3)
$p\,(x,t)$	holes per unit volume (1/cm^3)
$u\,(x,t)$	$n\,(x,t) - n\,(x,0)$, Excess electrons/unit volume
$u\,(x,t)$	$p\,(x,t) - p\,(x,0)$, Excess holes/unit volume
τ_p, τ_n	Minority carrier lifetime (s)
τ_1	minority carr. lifetime before neutron pulse (s)
τ_2	minority carr. lifetime after neutron pulse (s)
μ_p, μ_n	Minority carrier mobility (cm^2/Vs)
D, D_p, D_n	Minority carrier diffusion coefficient (cm^2/s)
D_a	$\frac{(n+p)D_nD_p}{nD_n+pD_p}$ Ambipolar diffusion (cm^2/s)
μ_a	$\frac{(n_0-p_0)\mu_n\mu_p}{n\mu_n+p\mu_p}$ Ambipolar mobility (cm^2/Vs)
τ_a	$\frac{p_0+u}{\tau_p(t)} - \frac{p_0}{\tau_{p0}} = \frac{n_0+u}{\tau_n(t)} - \frac{n_0}{\tau_{n0}}$ Ambipolar lifetime
L_p, L_n	$\sqrt{D_p\tau_p}$, $\sqrt{D_n\tau_n}$, Diffusion length (cm)
L	undepleted p or n width (cm)
W	depletion width (cm)
$\dot{\gamma}$	dose rate (rad(Si)/s)
$g\,(x,t)$, g_0	4.3x10$^{13}\dot{\gamma}$, generation density (1/cm^{3}s)
α_n	$n\pi/L$, Fourier sine series eigenvalue (1/cm)
$a_{i,n}$	$D(\alpha_n^2 + a^2 + \frac{1}{D\tau_i})$ sine series parameter (1/s)

recombination centers, decreasing carrier lifetime. The decrease in carrier lifetimes in doped semiconductor materials after exposure to a neutron fluence has been characterized as an abrupt decrease followed by a rapid short-term anneal (on the order of a few hours) and a long-term anneal (on the order of months), in which the carrier lifetime increases ([6]). Because the time scales associated with the annealing periods following a neutron pulse are very long in comparison to the length of a typical high-energy radiation (gamma) pulse, only an abrupt change in carrier lifetime is considered in this article. However, the general development of the next section allows an arbitrary time-dependent form of carrier lifetime.

The dynamics of neutron irradiation imply that the lattice damage and carrier lifetime degradation could be spatially dependent. To our knowledge, there is not a mathematical model describing this dependence. Our analysis assumes a spatially uniform carrier lifetime degradation; however, it may be possible to modify the analysis to a simple form of a spatially dependent lifetime. We do consider the possible spatial dependence of the excess carrier generation density. The resulting equations may be used to analyze the effects of a neutron irradiation on the photocurrent from an abrupt pn junction diode illuminated by monochromatic light, for example.

Fig. 1 shows a reverse-biased pn diode under light or ionizing radiation. We assume ohmic contacts at the device ends. The local coordinates are taken for convenience in the mathematical analysis. The photocurrent for the entire device consists of the sum of the depletion-zone photocurrent with the two minority carrier diffusion photocurrents from the undepleted regions [3]. For many reverse bias *pn* diodes in integrated-circuit (IC) applications, the depletion-zone photocurrent will be small in comparison with the diffusion currents and is ignored in this paper. A depletion-zone photocurrent analysis considering lifetime degradation from a neutron strike is given in [7].

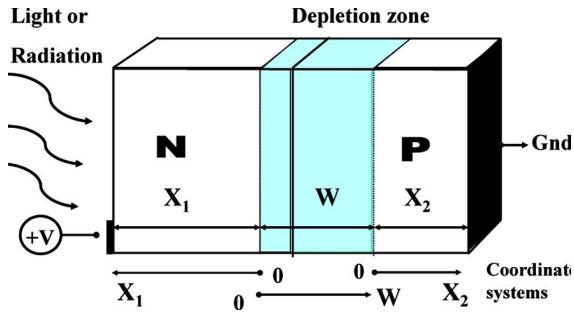

Fig. 1. Reverse-biased pn diode under light or ionizing irradiation. The device is irradiated from the left. For the 1-D analysis, the contacts are assumed to cover the entire left- and right-hand surfaces. The shaded region represents the depletion zone and the unshaded regions represent undepleted zones. The total current is the sum of the drift and diffusion current from the depleted and undepleted zones. Local coordinate systems are shown.

II. MATHEMATICAL DEVELOPMENT—SOLUTION TO THE 1-D AMBIPOLAR DIFFUSION EQUATION

In Cartesian coordinates under the assumption of charge neutrality, low-level gamma irradiation, and a time-dependent carrier lifetime, the 1-D ambipolar diffusion equation may be written as [1], [2]

$$u_t = D_a u_{xx} - \mu_a E u_x - \frac{u}{\tau_a(t)} + g(x,t);\ \ 0 \le x \le L,\ \ t > 0 \tag{1}$$

where $u(x,t)$ is the excess carrier density (n or p), and $g(x,t)$ is the excess carrier generation rate (in excess of the thermal carrier generation rate). The equations for the ambipolar coefficients D_a and μ_a and $\tau_a(t)$ are given in Table I. E is the electric field, composed of an internal field due to internal-charged carriers and an applied field due to an applied potential. We assume the boundary conditions at the contact and the edge of the depletion region are

$$u(0,t) = u(L,t) = 0 \tag{2}$$

with the initial condition $u(x,0) = f(x)$. L, the width of the undepleted region in which we solve the ADE, is constant as is W, the depletion width. The ambipolar carrier lifetime $\tau_a(t)$ is assumed to be a spatially uniform function of time in our analysis. Inherent in the derivation of the ambipolar diffusion equation is the assumption that the minority and majority carrier lifetimes are affected equally with respect to time. Specifically, [1, eq. 10.2–29] becomes

$$\tau_a(t) = \frac{p_0+u}{\tau_p(t)} - \frac{p_0}{\tau_{p_0}} = \frac{n_0+u}{\tau_n(t)} - \frac{n_0}{\tau_{n_0}} \tag{3}$$

where τ_{p_0} and τ_{n_0} are the average hole and electron carrier lifetimes, respectively, under preirradiation thermal equilibrium conditions. The quantities p_0 and n_0 are the concentrations of holes and electrons under preirradiation thermal equilibrium conditions. For low-level injection, $u(x,t)$ is much less than the majority carrier doping for the device, and the ambipolar coefficients become approximately those of the minority carrier

in the undepleted regions. Thus, for an n-type device under low-level irradiation, D_a, μ_a, and $\tau_a(t)$ become D_p, μ_p, and $\tau_p(t)$, respectively. From this point on, we further simplify our analysis by dropping subscripts, noting that D, μ, and $\tau(t)$ are associated with the minority carrier of each region. The current density is given by [1]

$$J(t) = \left[qD\frac{\partial u}{\partial x} \pm qu\mu E\right]\Bigg|_{x=0} \tag{4}$$

where $\pm$ is positive for the computation of J_p in n-type material and negative for the computation of J_n in p-type material. The leading sign on the right-hand side of the previous equation is chosen so that $J(t)$ is positive in our analysis.

The general solution to (1) is derived in Appendix A. It is

$$u(x,t) = \frac{2e^{ax}}{L}\sum_{n=1}^{\infty}\left[\bar{V}_n(0)e^{-D(\alpha_n^2+a^2)t-\int_0^t 1/\tau(s)ds}\right. \\ \left. + \int_0^t \bar{G}_n(w)e^{-D(\alpha_n^2+a^2)(t-w)-\int_w^t 1/\tau(s)ds}dw\right]\sin(\alpha_n x). \tag{5}$$

The definitions of a, α_n, $\bar{V}_n(0)$, and $\bar{G}_n(w)$ are given in Appendix A. Equation (5) represents the general solution for the excess carrier density. For the undepleted n-doped region, the corresponding current density evaluated at $x = 0$ is

$$J_p(t) = \frac{2qD}{L}\sum_{n=1}^{\infty}\alpha_n\left[\bar{V}_n(0)e^{-D(\alpha_n^2+a^2)t-\int_0^t 1/\tau(s)ds}+ \right. \\ \left. \int_0^t \bar{G}_n(w)e^{-D(\alpha_n^2+a^2)(t-w)-\int_w^t 1/\tau(s)ds}dw\right]. \tag{6}$$

The expressions given by (5) and (6) may be used to evaluate the excess carrier and current density distributions for an arbitrary function $\tau(s)$. In the case where the initial excess carrier density is zero at time $t = 0$, $\bar{V}_n(0) = 0$ and the first term is eliminated in the expressions. However, we note that the first term gives us a number of options in simulation. For example, we may stop a simulation and restart using the excess carrier density at the stopping time as the initial excess carrier density upon restart. Using this option, we may change parameters after stopping to approximate, in a piecewise linear fashion, nonlinear problems in which parameters change with respect to time. With careful consideration of charge conservation and changes in the depletion region boundary, we may also approximate moving boundary problems resulting from device bias changes during irradiation.

A. Special Cases

For the case of $g(x,t) = g(x)$ and $f(x) = 0$ (spatial variation only; no initial excess carriers), (5) reduces to

$$u(x,t) = \frac{2e^{ax}}{L}\sum_{n=1}^{\infty}\bar{G}_n \\ \times\left[\int_0^t e^{-D(\alpha_n^2+a^2)(t-w)-\int_w^t 1/\tau(s)ds}dw\right]\cdot\sin(\alpha_n x) \tag{7}$$

in which $\bar{G}_n$ is given by (30) in Appendix A. From (6), $J_p(t)$ becomes

$$J_p(t) = \frac{2qD}{L}\sum_{n=1}^{\infty}\bar{G}_n\alpha_n \\ \times\left[\int_0^t e^{-D(\alpha_n^2+a^2)(t-w)-\int_w^t 1/\tau(s)ds}dw\right]. \tag{8}$$

For the case where $g(x,t) = g(t)$ and $f(x) = 0$ (time variation only; no initial excess carriers), (5) reduces to

$$u(x,t) = \frac{2e^{ax}}{L}\sum_{n=1}^{\infty}\bar{w}_n\left[\int_0^t g(w)e^{-D(\alpha_n^2+a^2)(t-w)-\int_w^t 1/\tau(s)ds}dw\right] \\ \cdot\sin(\alpha_n x) \tag{9}$$

in which

$$\bar{w}_n = \int_0^L e^{-ax}\sin(\alpha_n x)dx \\ = \frac{\alpha_n\left(1-(-1)^n e^{-aL}\right)}{a^2+\alpha_n^2}. \tag{10}$$

From (6), we find

$$J_p(t) = \frac{2qD}{L}\sum_{n=1}^{\infty}\bar{w}_n\alpha_n \\ \cdot\left[\int_0^t g(w)e^{-D(\alpha_n^2+a^2)(t-w)-\int_w^t 1/\tau(s)ds}dw\right]. \tag{11}$$

When $E = 0$ and, therefore, $a = 0$, $\bar{w}_n = 0$ for n even and $\bar{w}_n = 2/\alpha_n$ for n odd. Under these conditions, any solution may be re-indexed to sum over only the odd terms, replacing the $\bar{w}_n$ term by $1/\alpha_{2n-1}$ and multiplying the leading coefficient of the series by a factor of 2 (see [7]).

B. Abrupt Change in Carrier Lifetime With $g(x,t) = g(t)$

A particular case of interest is that of an abrupt change in the carrier lifetime; $\tau(t) = \tau_1$, $t \le t'$ and $\tau(t) = \tau_2$, $t > t'$, for which the integral in the exponential terms becomes

$$\int_w^t \frac{1}{\tau(s)}ds = \begin{cases} \frac{t-w}{\tau_1}, & t\in[0,t') \\ \frac{t'-w}{\tau_1}+\frac{t-t'}{\tau_2}, & t\in[t',\infty),\ w\in[0,t') \\ \frac{t-w}{\tau_2}, & t\in[t',\infty),\ w\in[t',t] \end{cases} \tag{12}$$

so that

$$u(x,t) = \frac{2e^{ax}}{L}\sum_{n=1}^{\infty}\bar{w}_n I_n(t)\sin(\alpha_n x) \tag{13}$$

and from (11)

$$J_p(t) = \frac{2qD}{L}\sum_{n=1}^{\infty}\bar{w}_n\alpha_n I_n(t) \tag{14}$$

where

$$I_n(t) = \begin{cases} I_{1,n}(0,t); & 0\le t\le t' \\ e^{-a_{2,n}(t-t')}I_{1,n}(0,t')+I_{2,n}(t',t); & t>t' \end{cases} \tag{15}$$

and

$$I_{k,n}(a,b) = \int_a^b g(w) e^{-a_{k,n}(b-w)} dw \tag{16}$$

in which $a_{k,n} = D(\alpha_n^2 + a^2 + 1/D\tau_k)$.

C. Case 1: $g(t)$ is a Step Function, i.e., $g(x,t) = g_0$, $t > 0$

In this case, the evaluation of (15) gives

$$I_n(t) = \begin{cases} \frac{g_0(1-e^{-a_{1,n}t})}{a_{1,n}}; & 0 < t \le t' \\ \frac{g_0(1-e^{-a_{1,n}t'})e^{-a_{2,n}(t-t')}}{a_{1,n}} + \frac{g_0(1-e^{-a_{2,n}(t-t')})}{a_{2,n}}; & t' < t \end{cases}. \tag{17}$$

Substitution of (17) into either (13) or (14) provides us with the relevant solutions. The convergence rates of the two respective series may, however, be significantly improved by decomposing them into steady-state and transient components, and then replacing the steady-state series with the closed-form formulas given in Appendix B. The solution for $u(x,t)$ may then be written

$$u(x,t) = \begin{cases} u_{s,1}(x) - \frac{2g_0e^{ax}}{L}\sum_{n=1}^{\infty} \bar{w}_n \frac{e^{-a_{1,n}t}}{a_{1,n}} \sin(\alpha_n x); \\ \qquad 0 < t \le t' \\ u_{s,2}(x) + \frac{2g_0e^{ax}}{L}\sum_{n=1}^{\infty} \bar{w}_n \left[\frac{1-e^{-a_{1,n}t'}}{a_{1,n}} e^{-a_{2,n}(t-t')} - \right. \\ \left. \frac{e^{-a_{2,n}(t-t')}}{a_{2,n}}\right] \sin(\alpha_n x); \qquad t' < t \end{cases} \tag{18}$$

where

$$u_{s,k}(x) = g_0\tau_k \times \left[1 - e^{ax}\frac{(\sinh(\gamma_k(L-x)) + e^{-aL}\sinh(\gamma_k x))}{\sinh(\gamma_k L)}\right] \tag{19}$$

and $\gamma_k^2 = a^2 + 1/D\tau_k$. Applying the same technique to (14) using (17), we have

$$J_p(t) = \begin{cases} J_{s,1} - \frac{2qDg_0}{L}\sum_{n=1}^{\infty} \bar{w}_n \alpha_n \frac{e^{-a_{1,n}t}}{a_{1,n}}; \; 0 < t \le t' \\ J_{s,2} + \frac{2qDg_0}{L}\sum_{n=1}^{\infty} \bar{w}_n \alpha_n \left[\frac{1-e^{-a_{1,n}t'}}{a_{1,n}} e^{-a_{2,n}(t-t')} - \right. \\ \left. \frac{e^{-a_{2,n}(t-t')}}{a_{2,n}}\right]; \; t' < t \end{cases} \tag{20}$$

in which

$$J_{s,k} = qDg_0\tau_k \left[-a + \gamma_k \frac{(\cosh(\gamma_k L) - e^{-aL})}{\sinh(\gamma_k L)}\right]. \tag{21}$$

The terms $u_{s,k}(x)$ and $J_{s,k}$ represent the steady-state minority excess carrier and current densities with respect to the initial ($k = 1$) and final ($k = 2$) minority carrier lifetimes. We note that (18) and (20) agree with (18) and (19) of Axness *et al.* [5] for the case where there is no change in carrier lifetime ($\tau_1 = \tau_2$) (see [7]).

D. Case 2: $g(t)$ is a Square Pulse

In this case, the carrier lifetime is that of the previous section. The excess carrier generation density is defined by $g(x,t) = g_0(1 - H(t-t_1))$, where $H(t)$ denotes the Heaviside function. For the case where the neutron pulse occurs during the gamma irradiation ($t' < t_1$), we may evaluate $I_n(t)$ using (15) as

$$I_n(t) = \begin{cases} \frac{g_0\left(1-e^{-a_{1,n}t}\right)}{a_{1,n}}; & 0 < t \le t' \\ I_n(t')e^{-a_{2,n}(t-t')} + \frac{g_0\left(1-e^{-a_{2,n}(t-t')}\right)}{a_{2,n}}; & t' < t \le t_1 \\ I_n(t_1)e^{-a_{2,n}(t-t_1)}; & t > t_1 \end{cases}. \tag{22}$$

For the case where the neutron pulse occurs after the gamma irradiation ($t' > t_1$), we may evaluate $I_n(t)$ using (15) as

$$I_n(t) = \begin{cases} \frac{g_0\left(1-e^{-a_{1,n}t}\right)}{a_{1,n}}; & 0 < t \le t_1 \\ I_n(t_1)e^{-a_{1,n}(t-t_1)}; & t_1 < t \le t' \\ I_n(t')e^{-a_{2,n}(t-t')}; & t > t'. \end{cases} \tag{23}$$

As expected, both equations are the same as those for the step function except over the interval $t > t_1$. We note that (23) over the range $t > t_1$ takes the form of $I_n(t)$, evaluated at the previous endpoint multiplied by an exponential term dependent upon the time elapsed since that endpoint. The term $a_{k,n}$ in the exponential argument represents the rate of decrease of excess carriers for each eigenvalue taking into account losses through drift, diffusion, and recombination. This rate is dependent upon the minority carrier lifetime during which the elapsed time occurs ($k = 1$ for τ_1 and $k = 2$ for τ_2). Similar terms occur in (22). Over the range of $t' < t \le t_1$ in (22), the second term on the right-hand side represents the contribution of excess carriers produced during this period while the first term represents the contribution of carriers produced in the interval $0 < t \le t'$. The final equation for $t > t_1$ has the same form as (23). Finally, we note that semiclosed-form solutions for $u(x,t)$ and $J_p(t)$ may be obtained as derived in [7]. For $t' < t_1$, the results are

$$u(x,t) = \begin{cases} u_{s,1}(x) - \frac{2g_0e^{ax}}{L}\sum_{n=1}^{\infty} \bar{w}_n \frac{e^{-a_{1,n}t}}{a_{1,n}} \sin(\alpha_n x); \\ \qquad 0 < t \le t' \\ u_{s,2}(x) + \frac{2g_0e^{ax}}{L}\sum_{n=1}^{\infty} \bar{w}_n \left[\frac{1-e^{-a_{1,n}t'}}{a_{1,n}} e^{-a_{2,n}(t-t')} \right. \\ \left. - \frac{e^{-a_{2,n}(t-t')}}{a_{2,n}}\right] \sin(\alpha_n x); \qquad t' < t \le t_1 \\ \frac{2g_0e^{ax}}{L}\sum_{n=1}^{\infty} \bar{w}_n \left[\frac{1-e^{-a_{1,n}t'}}{a_{1,n}} e^{-a_{2,n}(t-t')} + \right. \\ \left. \frac{1-e^{-a_{2,n}(t_1-t')}}{a_{2,n}} e^{-a_{2,n}(t-t_1)}\right] \sin(\alpha_n x); \; t > t_1 \end{cases}$$

and

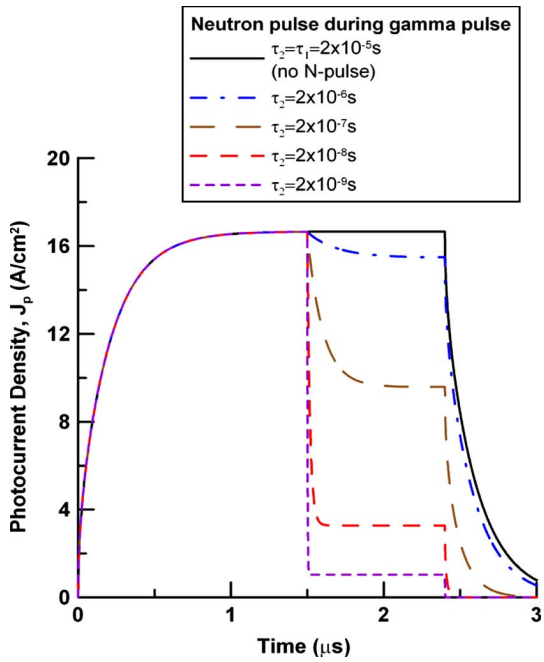

Fig. 2. Photocurrent from the undepleted n-doped region of a pn diode due to gamma irradiation with a concurrent neutron pulse. τ_1 is the prepulse minority carrier lifetime and τ_2 is the postneutron pulse minority carrier lifetime.

$$J_p(t)=\begin{cases} J_{s,1}-\frac{2qDg_0}{L}\sum_{n=1}^{\infty}\bar{w}_n\alpha_n\frac{e^{-a_{1,n}t}}{a_{1,n}}; & 0<t\le t' \\ J_{s,2}+\frac{2qDg_0}{L}\sum_{n=1}^{\infty}\bar{w}_n\alpha_n\left[\frac{1-e^{-a_{1,n}t'}}{a_{1,n}}e^{-a_{2,n}(t-t')}-\right. & \\ \left.\frac{e^{-a_{2,n}(t-t')}}{a_{2,n}}\right]; & t'<t\le t_1 \\ \frac{2qDg_0}{L}\sum_{n=1}^{\infty}\bar{w}_n\alpha_n\left[\frac{1-e^{-a_{1,n}t'}}{a_{1,n}}e^{-a_{2,n}(t-t')}+\right. & \\ \left.\frac{1-e^{-a_{2,n}(t_1-t')}}{a_{2,n}}e^{-a_{2,n}(t-t_1)}\right] & t>t_1 \end{cases}$$

where $u_{s,k}(x)$ and $J_{s,k}$ are given by (19) and (21). These terms represent the steady-state excess carrier and current densities. The equations for the case where $t'>t_1$ are given in [7].

As an example, we use the parameters of Fig. 2 in [5] to examine the photocurrent response in the undepleted n-type region of a pn diode due to a 2.4 μs square-wave gamma irradiation of 10^9 rad(Si)/s generation density. A neutron pulse is assumed to occur at 1.5 μs with a minority carrier lifetime degradation of one to four orders of magnitude. Other parameters were assigned as $L_p=0.015$, $\zeta_p=L/L_p=0.32$, and $\tau_p=2\times10^{-5}$ s. The ohmic field was set to zero. Similar pulse lengths are often used in testing. These parameters are typical for large devices, but smaller devices and shorter pulses will yield curves similar to Fig. 2. The gamma irradiation is assumed longer in this example than in [5, Fig. 2] to illustrate the dual steady-state behavior of the photocurrent.

Fig. 2 gives the analytic photocurrent density with respect to time for the aforementioned parameters. The top (solid) curve assumes the default minority carrier lifetime over the entire pulse length (no lifetime degradation). This curve is labeled $\tau_1=\tau_2=2\times10^{-5}$ s, where τ_1 is the minority carrier lifetime before the neutron pulse and τ_2 is the lifetime after the neutron pulse. The convergence to a steady current is evident. The photocurrent density curve directly below the top curve corresponds to the case where $\tau_2=2\times10^{-6}$ s. It is clear that this photocurrent shows a noticeable decrease when compared with the nondegraded photocurrent over the time spanned after the neutron pulse through the end of the gamma irradiation. The curves corresponding to degradations of two orders of magnitude or more show a more apparent decrease in photocurrent to a second steady state associated with this degraded carrier lifetime for the remainder of the gamma pulse. This example shows a dual steady-state behavior resulting from the degraded carrier lifetime.

E. Case 3: $g(t)$ is a Piecewise Linear Pulse

Experiments conducted at high-energy facilities generally measure the radiation generation density. Typically, the function describing this pulse is not a square wave, but may easily be described by a piecewise linear function with respect to time as shown in Fig. 3. For the two cases where the neutron pulse occurs during or after the gamma irradiation, we have evaluated $I_n(t)$ using (15). The derivation may be found in [7]. Using the expression for $I_n(t)$ and replacing the infinite series with closed-form formulas in some terms enables us to obtain a much faster convergence rate in the expressions for $u(x,t)$ and $J_p(t)$ (see [7]). The solutions may then be written

$$u(x,t)=\frac{2e^{ax}}{L}\cdot\begin{cases} [h_m(t-t_m)+g_m]S(x)_{1,1}-h_mS(x)_{1,2}+ & \\ \sum_{n=1}^{\infty}\bar{w}_nR_n(t)\sin(\alpha_nx); & 0\le t_m<t\le t'<t_{m+1} \\ [h_m(t-t_m)+g_m]S(x)_{2,1}-h_mS(x)_{2,2}+ & \\ \sum_{n=1}^{\infty}\bar{w}_nR_n(t)\sin(\alpha_nx); & t_m\le t'<t\le t_{m+1} \\ [h_s(t-t_s)+g_s]S(x)_{2,1}-h_sS(x)_{2,2}+ & \\ \sum_{n=1}^{\infty}\bar{w}_nR_n(t)\sin(\alpha_nx); & t_{m+1}<t_s<t\le t_{s+1}\le t_M \\ \sum_{n=1}^{\infty}\bar{w}_nR_n(t)\sin(\alpha_nx); & t>t_M \end{cases} \tag{24}$$

and

$$J_p(t)=\frac{2qD}{L}\begin{cases} [h_m(t-t_m)+g_m]S_{1,1}-h_mS_{1,2}+ & \\ \sum_{n=1}^{\infty}\bar{w}_n\alpha_nR_n(t); & 0\le t_m<t\le t'<t_{m+1} \\ [h_m(t-t_m)+g_m]S_{2,1}-h_mS_{2,2}+ & \\ \sum_{n=1}^{\infty}\bar{w}_n\alpha_nR_n(t); & t_m\le t'<t\le t_{m+1} \\ [h_s(t-t_s)+g_s]S_{2,1}-h_sS_{2,2}+ & \\ \sum_{n=1}^{\infty}\bar{w}_n\alpha_nR_n(t); & t_{m+1}<t_s<t\le t_{s+1}\le t_M \\ \sum_{n=1}^{\infty}\bar{w}_nR_n(t)\sin(\alpha_nx); & t>t_M \end{cases} \tag{25}$$

with $S(x)_{i,j}$, $S_{i,j}$, and $R_n(t)$ given in Appendix B. Since the expression for $g(t)$ is general in the aforementioned derivation, we may also compute $u(x,t)$ and $J_p(t)$ for the case where $t'>$

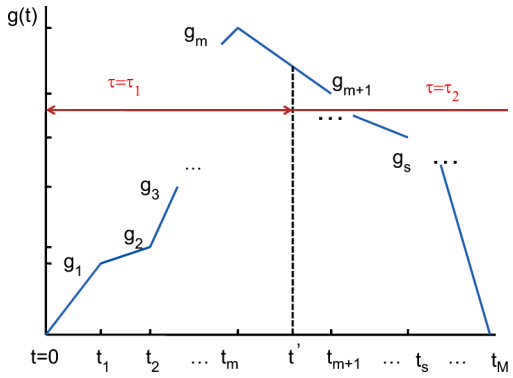

Fig. 3. Piecewise linear gamma irradiation generation density with a neutron pulse at $t = t'$. The pn diode minority carrier lifetime is $\tau = \tau_1$ for $t < t'$ and $\tau = \tau_2$ for $t \geq t'$.

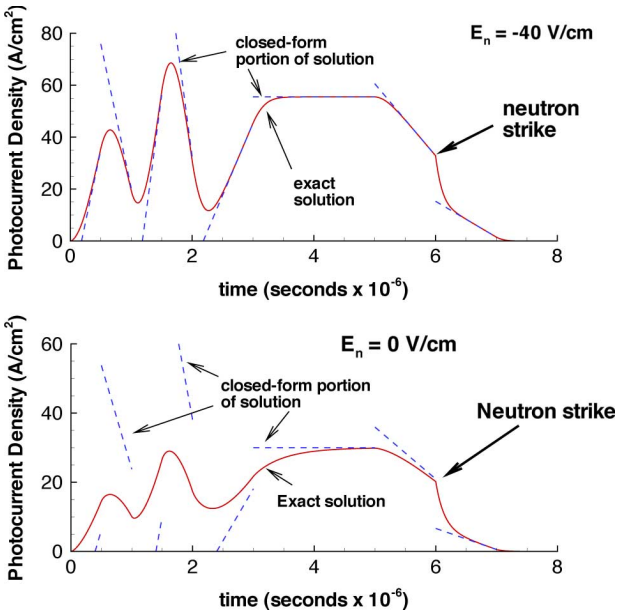

Fig. 4. Figure exhibiting minority current density behavior versus time from the undepleted n-doped region of an np diode for a negative ohmic field (top) and no ohmic field (bottom). The "closed-form" portions of the solutions are shown by the dashed line segments while the total current densities are given by continuous curves. Note the approach to the closed-form solution as time from the previous generation function endpoint increases. A high ohmic field of $E_n = -40$ V/cm was assumed in the upper plot to illustrate the bounding behavior of the closed-form part of the solution.

t_M by employing (24) and (25) and by introducing an additional segment to Fig. 3, upon which we define $g(t) = 0$ for $t_M < t \leq t' = t_{M+1}$.

In the case of the piecewise linear generation function, the closed-form portion of the current density consists of a set of line segments that bound the total current density when the number of terms in the computation is sufficiently large (about 50 terms). In the case where a negative ohmic field exists in the undepleted region, the current density approaches the line segments away from the generation function endpoints since the transient time-dependent exponential terms become small in these regions. In the case where there is no ohmic field, the current density does not necessarily approach the line segments, but the line segments bound the area in which the current density meanders. The behavior for both of these cases is shown in Fig. 4. For this figure, $g(t)$ is defined by the points $(t_i \times 10^{-6}$ s, $g_i \times 10^{22}$ pairs/cm^2/s) as (0, 0), (0.5, 5), (1, 0), (1.5, 8), (2, 0), (3, 5), (5, 5), and ($t_M = 7$, 0) (see Fig. 3). Other parameters are $t' = 6$ μs, $\tau_1 = 2 \times 10^{-5}$ s, $\tau_2 = 2 \times 10^{-7}$ s, $\mu_p = 461$ cm^2/Vs, $D_p = 11.91$ cm^2/s, and $L = 0.00764$ cm.

III. Conclusion

In this paper, we develop new solutions to the 1-D ambipolar diffusion equation (ADE) under low-level radiation conditions to approximate the photocurrent produced by a radiation pulse in the undepleted parts of an pn diode when the minority carrier lifetime is a function of time. Using Fourier sine series techniques developed in [8], we develop a general analytical solution to the 1-D ADE for the case where the excess carrier generation (a radiation or light pulse) is a function of time and space, which further simplifies when the excess carrier generation is either a function of time only or of space only. Solutions are developed for the occurrence of a neutron strike, which results in an instantaneous reduction of the carrier lifetimes within the device, either during or after a light or radiation pulse. The carrier lifetime is assumed to be spatially uniform within the device. For the particular case where the gamma pulse is time dependent only, the solution may be written as an infinite sum with each term consisting of the product of a time-dependent integral and a spatially dependent sine function. A number of cases are explored and illustrated with examples.

For the first case studied, the gamma irradiation is of the form of a step function $g(x,t) = g_0, t > 0$. In this case, the neutron pulse occurs during the gamma step function irradiation. The carrier lifetimes in each region of the pn diode instantaneously decrease at a time $t = t'$ and a reduction of current results that approaches a steady-state current dependent upon the decreased carrier lifetime. Equations are given in Section II-C.

For the second case, we assume that the gamma irradiation is of the form of a square pulse, with $g(x,t) = g_0, 0 < t \leq t_1$, and zero for $t > t_1$. The neutron pulse may occur during the gamma irradiation or while the device is recovering from the gamma pulse. The carrier and current densities are given for the undepleted n-type region of a pn diode with realistic parameters and a lifetime degradation spanning up to four orders of magnitude. The current densities are compared to those of a device with no carrier lifetime degradation for a neutron strike occurring during the gamma irradiation. For an order of magnitude degradation of the lifetime, only a small reduction in the photocurrent density is observed. For larger reductions in lifetime, very significant changes in the photocurrent occur. For long enough pulses, two steady states are observed, one associated with the original carrier lifetime and a second associated with the degraded carrier lifetime. In [7], we show the time history of the 1-D excess carrier density, which shows an abrupt decrease at the time associated with the lifetime degeneration. We also show an example problem where an ohmic field is present, which exhibits an extended current "tail" compared to the case of no ohmic field. For the case where there is no lifetime degradation, the equations are checked and found to be consistent with those of [5].

Finally, we solve the excess carrier and current densities for the case where $g(x,t) = g(t)$ is piecewise linear with respect to time and the abrupt change in lifetime occurs during or after

the pulse. This form of solution can be incorporated into circuit simulation codes, such as Xyce [9] or SPICE [10], and can be used to characterize the radiation sources at experimental facilities. The newly developed solutions have closed-form and infinite series components. The series components require only a few tens of terms for convergence with the accuracy increasing as we move away from the points t' and the endpoints of $g(t)$. Examples are shown for both a zero and large ohmic field.

Appendix A
General Solution of ADE Using the Finite Fourier Transform

We can solve the aforementioned boundary value problem via the substitution $u(x,t) = V(x,t)e^{ax}$, which will transform (1) to

$$V_t = DV_{xx} - \left(Da^2 + \frac{1}{\tau(t)}\right)V + g(x,t)e^{-ax} \tag{26}$$

where $a = \mu E/2D$. The transformed boundary conditions remain type I, homogeneous, while the initial condition becomes $V(x,0) = f(x)e^{-ax}$. The resulting boundary value problem may be solved by the finite Fourier sine transform [8]. That is, define

$$\bar{V}_n(t) = \int_0^L V(x,t)\sin(\alpha_n x)dx \tag{27}$$

with inversion formula

$$V(x,t) = \frac{2}{L}\sum_{n=1}^{\infty}\bar{V}_n(t)\sin(\alpha_n x) \tag{28}$$

in which $\alpha_n = n\pi/L$. Applying this transform to (26), yields the ODE

$$\frac{d}{dt}\bar{V}_n(t) + \left[D(\alpha_n^2 + a^2) + \frac{1}{\tau(t)}\right]\bar{V}_n(t) = \bar{G}_n(t); \quad n = 1,2,3\ldots \tag{29}$$

in which

$$\bar{G}_n(t) = \int_0^L g(x,t)e^{-ax}\sin(\alpha_n x)dx. \tag{30}$$

Applying the transform to the initial condition simply provides us with the initial condition for our ODE

$$\bar{V}_n(0) = \int_0^L f(x)e^{-ax}\sin(\alpha_n x)dx.$$

Therefore, the solution of our ODE is given by

$$\bar{V}_n(t) = \bar{V}_n(0)e^{-D(\alpha_n^2+a^2)t - \int_0^t 1/\tau(s)ds} + \int_0^t \bar{G}_n(w)e^{-D(\alpha_n^2+a^2)(t-w) - \int_w^t 1/\tau(s)ds}dw. \tag{31}$$

Substituting (31) into (28), we obtain $V(x,t)$. Therefore

$$u(x,t) = \frac{2e^{ax}}{L}\sum_{n=1}^{\infty}\left[\bar{V}_n(0)e^{-D(\alpha_n^2+a^2)t - \int_0^t 1/\tau(s)ds} + \int_0^t \bar{G}_n(w)e^{-D(\alpha_n^2+a^2)(t-w) - \int_w^t 1/\tau(s)ds}dw\right]\sin(\alpha_n x). \tag{32}$$

Appendix B
Steady-State Formulas

The aforementioned steady-state formulas, which appear in Section II, are presented below. A more detailed derivation is given in [7]. In brief, using Fourier expansion formulas (see [11, p. 13]), it can be shown that

$$S(x)_{k,1} = \sum_{n=1}^{\infty}\frac{\bar{w}_n\sin(\alpha_n x)}{a_{k,n}} = \frac{L\tau_k}{2}\left[e^{-ax} - \frac{\sinh(\gamma_k(L-x)) + e^{-aL}\sinh(\gamma_k x)}{\sinh(\gamma_k L)}\right]; \quad (0 \le x \le L) \tag{33}$$

in which $\gamma_k^2 = a^2 + 1/D\tau_k$. Differentiating (33) with respect to x , then replacing each x with zero, reveals that

$$S_{k,1} = \sum_{n=1}^{\infty}\frac{\bar{w}_n\alpha_n}{a_{k,n}} = \frac{L\tau_k}{2}\left[-a + \frac{\gamma_k\left(\cosh(\gamma_k L) - e^{-aL}\right)}{\sinh(\gamma_k L)}\right]. \tag{34}$$

Then, differentiating (33) and (34) with respect to τ_k, we find

$$\begin{aligned} S(x)_{k,2} = \sum_{n=1}^{\infty}\frac{\bar{w}_n\sin(\alpha_n x)}{(a_{k,n})^2} &= \frac{L\tau_k^2}{2}\left[e^{-ax} - \frac{\left(\sinh(\gamma_k(L-x)) + e^{-aL}\sinh(\gamma_k x)\right)}{\sinh(\gamma_k L)}\right] \\ &+ \frac{L\tau_k}{4D\gamma_k\sinh^2(\gamma_k L)}\Big[L\sinh(\gamma_k x) - \\ &x\sinh(\gamma_k L)\cosh(\gamma_k(L-x)) \\ &+ e^{-aL}\left(x\sinh(\gamma_k L)\cosh(\gamma_k x)\right. \\ &\left. -L\sinh(\gamma_k x)\cosh(\gamma_k L)\right)\Big]; \; 0 \le x \le L \end{aligned} \tag{35}$$

and

$$\begin{aligned} S_{k,2} = \sum_{n=1}^{\infty}\frac{\bar{w}_n\alpha_n}{(a_{k,n})^2} &= \frac{L\tau_k^2}{2}\left[-a + \gamma_k\frac{\left(\cosh(\gamma_k L) - e^{-aL}\right)}{\sinh(\gamma_k L)}\right] \\ &- \frac{L\tau_k}{4D\gamma_k\sinh^2(\gamma_k L)} \\ &\times\Big[\sinh(\gamma_k L)\cosh(\gamma_k L) - e^{-aL}\sinh(\gamma_k L) \\ &- \gamma_k L + \gamma_k L\cosh(\gamma_k L)e^{-aL}\Big]. \end{aligned} \tag{36}$$

Formulas (34) and (36) are required for computing $J_p(t)$ while (33) and (35) are required for computing $u(x,t)$. $R_n(t)$ is given by

$$R_n(t) = \begin{cases} \frac{1}{a_{1,n}}\left[\sum_{i=0}^{m-1}\left[\left(g_{i+1}-\frac{h_i}{a_{1,n}}\right)e^{-a_{1,n}(t-t_{i+1})}- \left(g_i-\frac{h_i}{a_{1,n}}\right)e^{-a_{1,n}(t-t_i)}\right]-\left(g_m-\frac{h_m}{a_{1,n}}\right)e^{-a_{1,n}(t-t_m)}\right] \\ 0\le t_m<t\le t'<t_{m+1}; \\ I_n(t')e^{-a_{2,n}(t-t')}-\frac{1}{a_{2,n}}\cdot \\ \left\{\left(h_m(t'-t_m)+g_m-\frac{h_m}{a_{2,n}}\right)e^{-a_{2,n}(t-t')}\right\}; \\ t_m\le t'<t\le t_{m+1} \\ I_n(t_{m+1})e^{-a_{2,n}(t-t_{m+1})}+\frac{1}{a_{2,n}}\left\{\sum_{i=m+1}^{s-1}\left[\left(g_{i+1}-\frac{h_i}{a_{2,n}}\right)\cdot e^{-a_{2,n}(t-t_{i+1})}-\left(g_i-\frac{h_i}{a_{2,n}}\right)e^{-a_{2,n}(t-t_i)}\right] \right. \\ \left. -\left(g_s-\frac{h_s}{a_{2,n}}\right)e^{-a_{2,n}(t-t_s)}\right\}; \\ t_{m+1}<t_s<t\le t_{s+1}\le t_M \\ I_n(t_M)e^{-a_{2,n}(t-t_M)};t>t_M \end{cases}.$$

REFERENCES

[1] J. P. McKelvey, *Solid State and Semiconductor Physics*. Malabar, FL: Robert E. Krieger, 1966.

[2] W. van Roosbroeck, *Phys. Rev.*, vol. 91, p. 282, 1953.

[3] J. L. Wirth and S. C. Rogers, "The transient response of transistors and diodes to ionizing radiation," *IEEE Trans. Nucl. Sci.*, vol. NS-11, no. 5, pp. 24–38, Nov. 1964.

[4] O. M. Stuetzer, *Extended Steady-State Analysis of the Gamma-Irradiated Cartesian P-N Junction, SAND86-7174*. Albuquerque, NM: Sandia National Laboratories, 1987.

[5] C. L. Axness, B. Kerr, and T. F. Wunsch, "Analytic light- or radiation-induced pn junction photocurrent solutions to the multidimensional ambipolar diffusion equation," *J. Appl. Phys.*, vol. 96, no. 5, Sep. 2004.

[6] J. R. Srour, C. J. Marshall, and P. W. Marshall, "A review of displacement damage effects in silicon devices," *IEEE Trans. Nucl. Sci.*, vol. 50, no. 3, pp. 653–670, Jun. 2003.

[7] B. Kerr, C. L. Axness, and E. R. Keiter, *Analytic 1D pn Junction Diode Photocurrent Solutions Following Ionizing Radiation and Including Time-Dependent Changes in the Carrier Lifetime From a Non-Concurrent Neutron Pulse, SAND2010-3284*. Albuquerque, NM: Sandia National Laboratories, 2010.

[8] M. N.Özisik, *Boundary Value Problems of Heat Conduction*. Scranton, PA: International Textbook Co., 1968.

[9] H. K. Thornquist, E. R. Keiter, R. J. Hoekstra, D. M. Day, and E. G. Boman, "A parallel preconditioning strategy for efficient transistor-level circuit simulation," presented at the IEEE/ACM International Conf. Computer-Aided Design-Digest of Technical Papers, San Jose, CA, Nov. 2–5, 2009.

[10] L. W. Nagel, *SPICE2: A Computer Program to Simulate Semiconductor Circuits, ERL Memo No. ERL-M5250*. Berkeley, CA: Electronics Research Lab., Univ. California, 1975.

[11] F. Oberhettinger, *Fourier Expansions*. New York: Academic Press, 1973.